ISSN(PRINT) : 2320 -1967
ISSN(ONLINE) : 2320 -1975

GLOBAL SCIENTIFIC INC.

ChemXpress

ORIGINAL ARTICLE

CHEMXPRESS 5(3), 089-097, (2014)

Structure and internal dynamics of 1,2-propanediammonium pentachloroantimonate (III) dichloride of formula $[C_3H_{10}N_2]_2Cl_2SbCl_5$

Mohsen Ouled Mohamed Sghaier*[1], Krystyna Holderna-Natkaniec[2], Piotr Czarnecki[2], Slaheddine Chaabouni[1]

[1]Laboratory of Materials Science and Environment, Faculty of Sfax, BP 1171, 3000 Sfax, (TUNISIA)
[2]Department of Physics Adam Mickiewicz University, 61-614 Poznan Umultowska 85, (POLAND)
E-mail : mohsenesghaier@yahoo.fr; natkanie@amu.edu.pl; pczarnec@amu.edu.pl; chaabouni_slaheddine@yahoo.fr

Received : 08th April, 2014 ; Revised : 08th June, 2014 ; Accepted : 11th June, 2014

Abstract : 1,2-propanediammonium pentachloroantimonate (III) dichloride, PDA, has been synthesized and characterized by the X-ray at 293K. It crystallize in the orthorhombic space group, P212121 with the following unit-cell dimensions: a = 9.2610(7)Å, b = 10.5950(6)Å, c = 19.4830(1)Å and Z = 4. The crystal structure consists of 1,2-propanediammonium cations, $[SbCl_5]^{2-}$ anions and two frees atoms chlor. The Sb III atom is coordinated by six Cl atoms which form one-dimensional infinite chains of composition $[SbCl_6]^{3-}$. The compound is stabilized by intermolecular N—H….Cl hydrogen bonds. The dynamics of the proton and the molecular motion revealed the phase transitions at the vicinity of 261K and 355K.

Keywords : Crystal structure; Internal dynamics.

INTRODUCTION

Halogenoantimonates(III) and halogenobismuthates(III) with organic cations defined by the general formula $(RNH_3^+)_n(M_mX_{n+3m})^{n-}$ (where M is SbIII, BiIII; X is Cl, Br, I) are an interesting group of compounds due to their ferroelectric properties[1-4]. The polarity of these crystals is associated with phase transitions, which are mainly caused by the changes in rotational motions of the organic cations[2,5]. These phenomena are especially manifested in the structures containing relatively small methyl-, dimethyl-, trimethyl- and tetramethylammonium cations[2,6-9]. Differences in the size, symmetry and ability to form hydrogen bonds of the various possible organic cations, together with the many different possible metal-halogen atom configurations, provide a rich family of compounds. The anionic structures that have been reported so far range from simple isolated $[MX_6]^{3-}$ octahedra and $[MX_5]^{2-}$ square pyramids through isolated units containing oc-

ORIGINAL ARTICLE

tahedra/square pyramids, connected by corners, edges or faces, to infinite one- or two-dimensional polyanionic structures[10,11]. In this paper we report the synthesis, crystal structure, and internal dynamics of PDA.

EXPERIMENTAL

Single crystals of $[C_3H_{12}N_2]_2Cl_2SbCl_5$ were obtained in the reaction of $SbCl_3$ (1ml) with 1-2 diaminopropane (1.187ml) with a large excess of HCl (5ml) in the presence of ethanol. The synthesized compound was purified by repeated crystallizations. Transparent single crystals were grown at room temperature, and had the form of prism.

Intensity data were collected using a CAD4 Express diffractometer with graphite-monochromated (Mo K α) at 293 K. The positional parameters for the heavy atoms were obtained from a three-dimensional Patterson map, while the non- hydrogen atoms were found from successive difference Fourier Maps. The structure was refined by full-matrix least squares using anisotropic temperature factors for all non-hydrogen atoms and the hydrogen atoms were localized and optimized to restraint positions. Calculations were performed with the SHELXS-86 program[12], using the scattering factors enclosed therein. The crystal data, collected reflections and parameters of the final refinement are reported in TABLE 1. Final atomic coordinates and equivalent isotropic displacement parameters for the atoms are shown in TABLE 2. List of atomic displacement parameters are shown in TABLE 3.

The thermals parameters of the polycrystalline sample were carried out on a differential scanning calorimeter DSC Q2000 TA Instruments, on heating the sample from 95K to 490K and cooling down to 95 K. Aluminum sample pans were used with sample weights of 7 mg. All operations were performed at a rate of 10 K/min in a nitrogen atmosphere using an empty aluminum sample pan as the reference.

The first derivative of absorption signal from the radio frequency (r.f.) field was recorded on a laboratory made instrument operating in the double modulation system, by a linear change in the frequency of the autodyne generator within the range from 25.42 to 25.66 MHz at a constant magnetic field of 0.6 T stabilized by F^{19} NMR system. The signal was averaged and corrected for the amplitude of the second modulation. The measurements were performed on heating the sample from 60 K to 520 K.

RESULTS AND DISCUSSION

Single-crystal x-ray diffraction experiment

1,2-propanediammonium pentachloroantimonate (III) dichloride crystallizes at room temperature in the orthorhombic $P2_12_12_1$ space group. The projection of the crystal structure of $[C_3H_{10}N_2]_2Cl_2SbCl_5$ along the a direction is presented in Figure 1. The anionic sublattice is composed of $[SbCl_6]^{3-}$ deformed octahedra. They are connected at the corners forming polymeric one-dimensional chains extending along the a-axis (Figure 1). Each octahedron possesses two bridging and four terminal chlorine atoms. The Sb–Cl

TABLE 1 : Crystal and experimental data

Chemical formula:	$C_6 H_{24} Cl_7 N_4 Sb_1$
Formula weight (g mol^{-1})	522.20
T = 293	
Crystal color; habit	white; prism
Crystal size (mm^3)	0.42*0.22*01
Crystal system	Orthorhombic
Space group	P212121
Unit cell dimensions (Å)	a = 9.2610(7)
	b = 10.5950(6)
	c = 19.4830(1)
Volume($Å^3$)	1911.9304(2)
Z	4
Density (calculated) (g cm^{-3})	1.814
Wavelength (Å)	AgKa, λ = 0.56087
Absorption coefficient (mm^{-1})	1.254
F(0 0 0)	1032
θ Range (deg.)	2.241-27.963
Index ranges	$0 \le h \le 15$; $0 \le k \le 17$; $-5 \le l \le 32$
Reflections collected/unique	6383/6183 (Rint = 0.0140)
Observed reflections [I□2σ (I)]	2220
Data/parameters	2220/164
Goodness of fit on F^2	0.9990
Final R indices [I□2σ (I)][a]	R_1 = 0.0261, wR_2 = 0.0284
R indices (all data)[a]	R_1 = 0.0261, wR_2 = 0.0284
Largest diff. peak/hole (e $Å^{-3}$)	1.44/-1.12
CCDC deposite number: 870885	

TABLE 2 : Atomic coordinates and equivalent isotropic displacement parameters (Å²) of PDA

Atom	x	y	z	U_{eq}[Å²]	Atom	x	y	z	U_{eq}[Å²]
Sb1	0.32280(3)	0.21583(3)	0.76573(2)	0.0262	H41	1.0022	0.3004	0.9592	0.0500
Cl1	0.35772(19)	0.23599(16)	0.90167(8)	0.0478	H42	1.0336	0.2633	0.8889	0.0500
Cl2	0.51451(15)	0.97128(14)	0.76138(9)	0.0412	H43	1.0043	0.1676	0.9405	0.0500
Cl3	0.14133(14)	0.05737(12)	0.78629(9)	0.0381	C11	0.6383(6)	0.2770(6)	0.5696(3)	0.0372
Cl4	0.27346(18)	0.21325(19)	0.63847(8)	0.0480	H111	0.7031	0.2598	0.5316	0.0500
Cl5	0.13309(14)	0.37345(12)	0.77857(9)	0.0381	H112	0.5402	0.2599	0.5543	0.0500
Cl6	0.60053(16)	0.00346(14)	0.00572(9)	0.0428	C12	0.6759(7)	0.1946(5)	0.6301(3)	0.0360
Cl7	0.04781(17)	0.96914(15)	0.97502(9)	0.0455	H121	0.6103	0.2156	0.6680	0.0500
N1	0.6496(5)	0.4120(5)	0.5890(3)	0.0367	C13	0.6455(6)	0.0607(4)	0.6097(3)	0.0285
H11	0.6285	0.4606	0.5535	0.0500	H131	0.6686	0.0053	0.6471	0.0500
H12	0.7402	0.4281	0.6028	0.0500	H132	0.7052	0.0389	0.5707	0.0500
H13	0.5895	0.4283	0.6236	0.0500	H133	0.5462	0.0513	0.5975	0.0500
N2	0.8291(8)	0.2087(6)	0.6548(4)	0.0667	C21	0.7853(7)	0.1565(7)	0.8532(4)	0.0447
H21	0.8457	0.1580	0.6905	0.0500	H211	0.6882	0.1756	0.8368	0.0500
H22	0.8455	0.2886	0.6677	0.0500	H212	0.8504	0.1706	0.8144	0.0500
H23	0.8911	0.1891	0.6211	0.0500	C22	0.8226(7)	0.2494(5)	0.9098(3)	0.0343
N3	0.7935(6)	0.0235(5)	0.8743(3)	0.0476	H221	0.7687	0.2288	0.9505	0.0500
H31	0.7680	-0.0252	0.8392	0.0500	C23	0.7818(8)	0.3813(7)	0.8881(5)	0.0549
H32	0.7328	0.0112	0.9091	0.0500	H231	0.8089	0.4403	0.9243	0.0500
H33	0.8827	0.0059	0.8872	0.0500	H232	0.6804	0.3865	0.8809	0.0500
N4	0.9821(6)	0.2456(4)	0.9261(3)	0.0394	H233	0.8325	0.4046	0.8470	0.0500

TABLE 3 : Atomic displacement parameters (Å²) of PDA

Atom	U^{11}	U^{22}	U^{33}	U^{23}	U^{13}	U^{12}
Sb1	0.02411(10)	0.02381(10)	0.03061(14)	0.00091(16)	0.00239(15)	0.00033(13)
Cl1	0.0600(9)	0.0471(8)	0.0363(7)	-0.0008(7)	-0.0079(7)	0.0013(7)
Cl2	0.0374(6)	0.0452(6)	0.0411(8)	0.0019(8)	0.0037(7)	0.0047(5)
Cl3	0.0316(6)	0.0327(5)	0.0500(9)	0.0018(6)	0.0018(6)	-0.0078(4)
Cl4	0.0651(9)	0.0459(7)	0.0329(7)	-0.0009(9)	-0.0027(7)	-0.0046(8)
Cl5	0.0325(6)	0.0317(5)	0.0501(10)	0.0041(6)	0.0053(6)	0.0107(4)
Cl6	0.0403(7)	0.0435(7)	0.0446(8)	-0.0052(7)	-0.0070(7)	0.0045(6)
Cl7	0.0419(7)	0.0471(7)	0.0476(9)	0.0103(7)	0.0099(7)	0.0089(6)
N1	0.035(2)	0.033(2)	0.042(3)	0.004(2)	0.002(2)	0.0006(18)
N2	0.079(4)	0.046(3)	0.075(4)	0.002(4)	-0.034(4)	0.010(4)
N3	0.052(3)	0.043(3)	0.047(3)	-0.013(3)	0.003(3)	-0.013(2)
N4	0.041(2)	0.029(2)	0.048(3)	-0.008(2)	-0.008(2)	-0.0022(17)
C11	0.038(2)	0.031(2)	0.043(3)	0.001(3)	-0.009(2)	0.001(2)
C12	0.045(2)	0.032(2)	0.031(2)	0.000(2)	0.001(3)	0.001(3)
C13	0.037(3)	0.0201(18)	0.028(2)	-0.0012(19)	-0.005(2)	-0.0040(17)
C21	0.049(4)	0.047(3)	0.037(3)	-0.007(3)	-0.007(3)	0.001(3)
C22	0.033(2)	0.033(2)	0.037(3)	-0.001(2)	0.002(3)	0.002(2)
C23	0.045(4)	0.041(3)	0.078(6)	0.007(4)	0.006(4)	0.010(3)

ORIGINAL ARTICLE

bond lengths fall into three ranges: the longest bonds (3.1425(15)–3.1424(14)Å) are characteristic of bridging halogen atoms, and the shortest (2.4092(13)–2.4370(12)Å) of terminal bonds opposite to the bridging, while those neither terminal nor bridging have intermediate lengths (2.5213(16)–2.6768(17)Å) (TABLE 4). The Cl–Sb–Cl angles for atoms *cis* to each other are between 86.04(6) and 92.27(5)°, while the *trans* angles are 115.77(10)°, 164.30(4)°, 167.23(4)° and 174.74(6)°. This coordination is similar to that found in other chloroantimonate(III) crystals in which anionic substructures are also built of polymeric $[(SbCl5)_n]^{2n-}$ chains, e.g.[13-16]. The 1,2-propane ammonium cations are found between the ionic chains with two chlorine atom, this are linked to this inorganic $[(SbCl5)_n]^{2n-}$ chains through the N–H…Cl hydrogen bonds (TABLE 5), and are thus partly responsible for the distorted octahedral coordination of the SbIII, both in terms of differences between equivalent Sb–Cl distances and Cl–Sb–Cl angles. The influence of these intermolecular interactions is clearly seen in the geometrical parameters involving the weakest-bonded bridging chlorine atoms (Figure 2). The presence of relatively strong hydrogen bonds partly causes significant distortion of the inter-octahedral $Sb1^{iv}$–Cl2–$Sb1^{iii}$ angle (170.30(6)°) from its ideal value of 180°[17]

TABLE 4 : Selected bond lengths (Å) and angles (°) for PDA

Atom	bond lengths (Å)	Atom	Angles (°)
Sb1-Cl1	2.6768(17)	Cl1-Sb1-Cl5	86.04(6)
Sb1-$Cl2^{i}$	3.1424(14)	$Cl2^{i}$-Sb1-Cl1	91.39(5)
Sb1-$Cl2^{ii}$	3.1425(15)	$Cl2^{ii}$-Sb1-Cl1	92.27(5)
Sb1-Cl3	2.4092(13)	$Cl2^{i}$-Sb1-$Cl2^{ii}$	115.770(10)
Sb1-Cl4	2.5213(16)	$Cl2^{i}$-Sb1-Cl3	79.86(4)
Sb1-Cl5	2.4370(12)	$Cl2^{ii}$-Sb1-Cl3	164.30(4)
N1-C11	1.483(8)	$Cl2^{i}$-Sb1-Cl4	93.84(6)
C12-C11	1.509(8)	$Cl2^{ii}$-Sb1-Cl4	86.04(5)
C12-N2	1.505(10)	$Cl2^{i}$-Sb1-Cl5	167.23(4)
C12-C13	1.500(7)	$Cl2^{ii}$-Sb1-Cl5	76.86(4)
N3-C21	1.470(9)	Cl3-Sb1-Cl1	88.59(6)
C22-C21	1.518(8)	Cl3-Sb1-Cl4	91.69(6)
C22-N4	1.511(8)	Cl3-Sb1-Cl5	87.57(4)
C22-C23	1.509(8)	Cl4-Sb1-Cl1	174.74(6)
		Cl4-Sb1-Cl5	88.72(6)
		$Sb1^{iii}$-Cl2-$Sb1^{iv}$	170.30(6)
		C11-C12-C13	107.2(5)
		C11-C12-N2	114.2(5)
		C12-C11-N1	110.0(5)
		C13-C12-N2	110.9(5)
		C21-C22-C23	109.9(6)
		C21-C22-N4	111.0(5)
		N4-C22-C23	109.1(5)
		C22-C21-N3	113.9(5)

Symmetry codes: (i) x, -1+y, z; (ii) 1-x, -0.5+y, 1.5-z; (iii) x, 1+y, z; (iv) 1-x, 0.5+y, 1.5-z

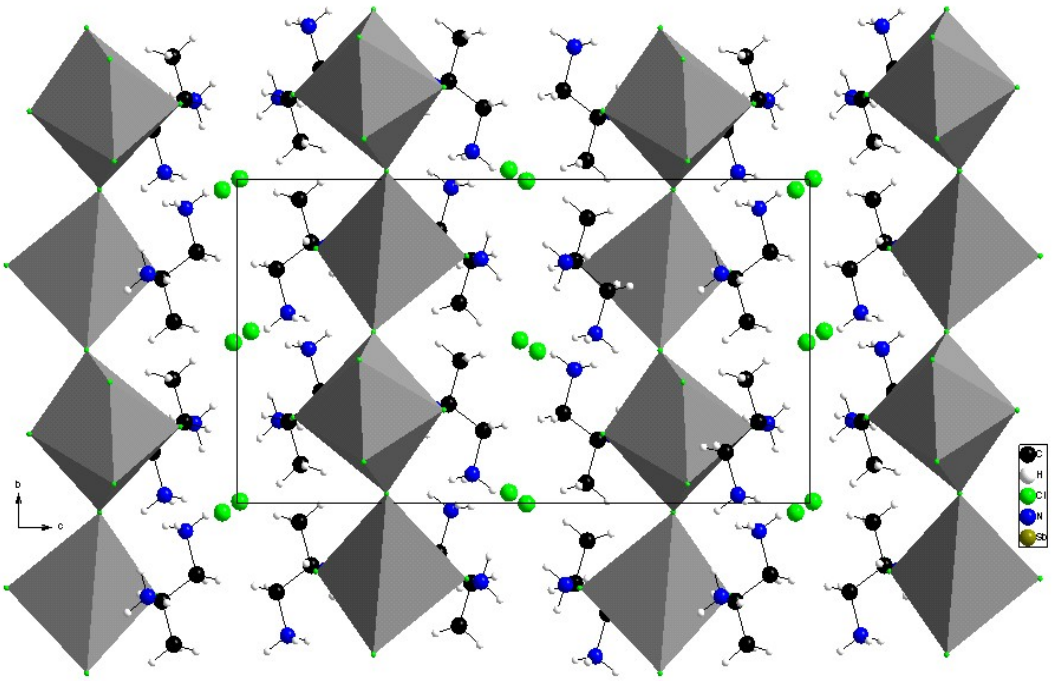

Figure 1 : The projection of the crystal structure along the a-axis.

ORIGINAL ARTICLE

Differential scanning calorimetry

The thermal analysis result is reported in Figure 3. The thermogram shows two endothermic peaks at the vicinity of 261K and 355K, while the melting point was not obtain.

TABLE 5 : Hydrogen-bond geometry (Å, °).

D-H…A	d(D-H)	d(H...A)	D-H…A	d(D...A)
N1-H11…Cl6^{i}	0.890	2.457	132.08	3.124
N1-H12…Cl7^{ii}	0.890	2.519	125.72	3.123
N1-H12…Cl3^{iii}	0.890	2.786	133.84	3.462
N1-H13…Cl2^{ii}	0.890	2.481	163.43	3.344
N2-H22…Cl3^{iii}	0.890	2.988	173.37	3.874
N3-H31…Cl5^{ii}	0.890	2.696	142.99	3.448
N3-H31…Cl2$_{iv}$	0.890	2.793	129.96	3.434
N3-H31…Cl4^{ii}	0.890	2.833	119.49	3.362
N3-H32…Cl6^{v}	0.890	2.247	170.85	3.129
N3-H33…Cl7^{vi}	0.890	2.330	149.15	3.128
N4-H41…Cl6^{vii}	0.890	2.370	150.17	3.173
N4-H42…Cl5^{viii}	0.890	2.612	163.17	3.473
N4-H43…Cl7^{vi}	0.890	2.242	176.91	3.131

Symmetry codes: (i) -x+1, y+1/2, -z+1/2; (ii) -x+1, y-1/2, -z+3/2; (iii) -x+1, y+1/2, -z+3/2; (iv) x, y-1, z; (v) x, y, z+1; (vi) x+1, y-1, z, (vii) x+1/2, -y+1/2, -z+1; (viii) x+1, y, z

^{1}H NMR measurements

The ^{1}H NMR spectra of the PDA were recorded in the temperature range from 60 K to 520K. Figure 4 gives exemplary ^{1}H NMR spectra taken at different temperatures. In the low temperature phase a narrowing of the broad line on heating is observed. The maximum slope line width decreased from 22.7 at 60 K to 11.7 at 150 K. Above the temperature of T=157 K, a narrow component of the line appears. Its intensity increased above the characteristic temperature at T=261K and wide component narrows above 355 K. At the melting point the line width is close to zero, i.e. it is of an order of the magnetic field inhomogeneity.

The second moment of ^{1}H NMR line is usually used to characterize the absorption signal in r.f. field. The second moment of the ^{1}H NMR line, M_2, at some temperatures was calculated according to the formula[18]:

$$M_2 = \frac{1}{3}\frac{\int_0^{\infty}(H - H_0)^2 f'(H)dH}{\int_0^{\infty} f'(H)dH} \quad (1)$$

by numerical integration of the first derivative of the absorption signal $f'(H)$. The second moment of ^{1}H NMR line was $40\cdot10^{-8}$ T^2 at 60 K, and on heating it

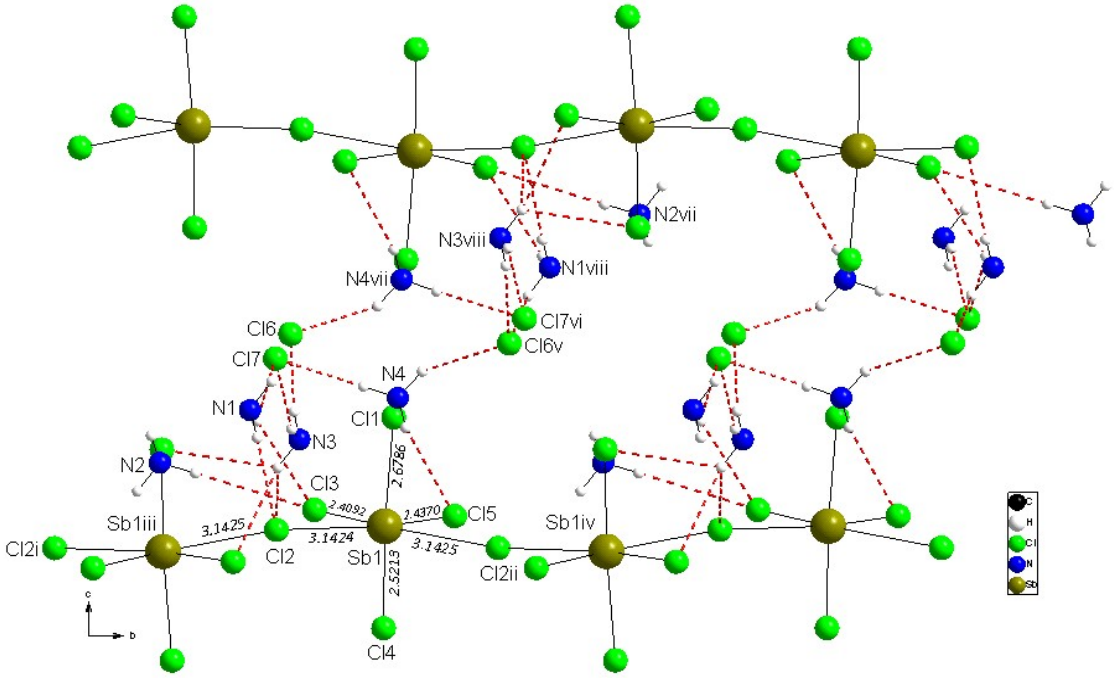

Figure 2 : The N–H…Cl hydrogen bonds (thin dashed lines) involving Cl2, Cl3, Cl4 and Cl5 atoms that partly contribute to the deformation of the [SbCl6]$^{3-}$ octahedron in the structure of PDA. Symmetry codes: (i) -x+1, y+1/2, -z+1/2; (ii) -x+1, y-1/2, -z+3/2; (iii) -x+1, y+1/2, -z+3/2; (iv) x, y-1, z (v) x, y, z+1; (vi) x+1, y-1, z, (vii) x+1/2, -y+1/2, -z+1; (viii) x+1, y, z.

ORIGINAL ARTICLE

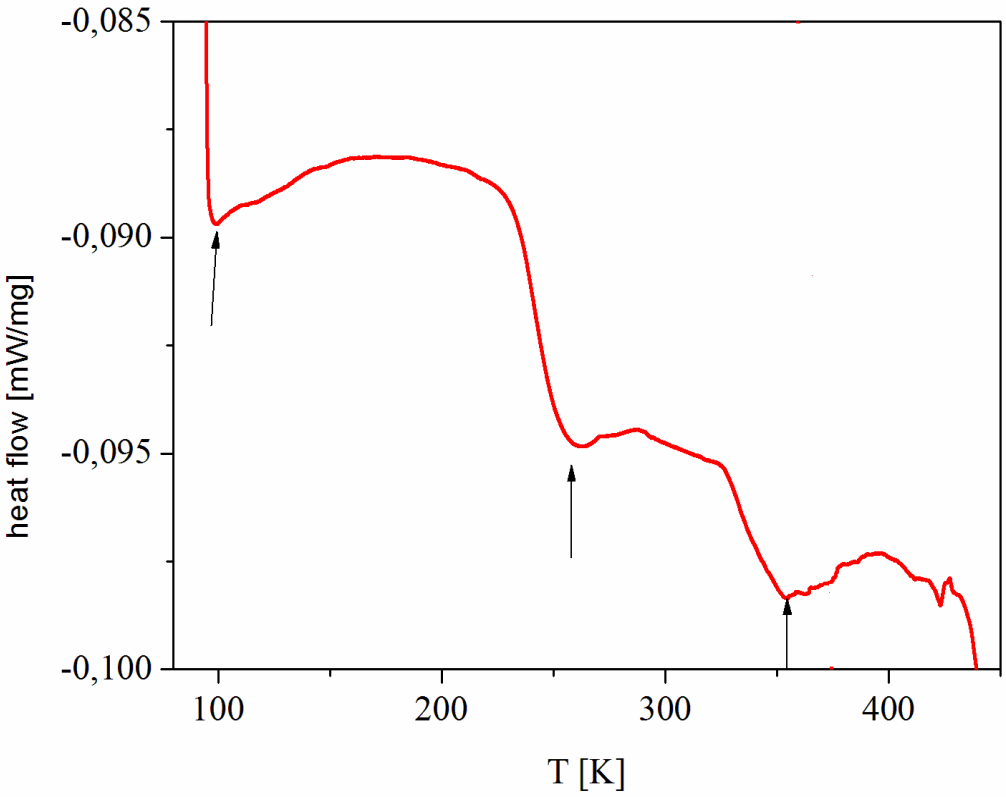

Figure 3 : The DSC thermogram of $[C_3H_{12}N_2]_2Cl_2SbCl_5$ recorded on heating.

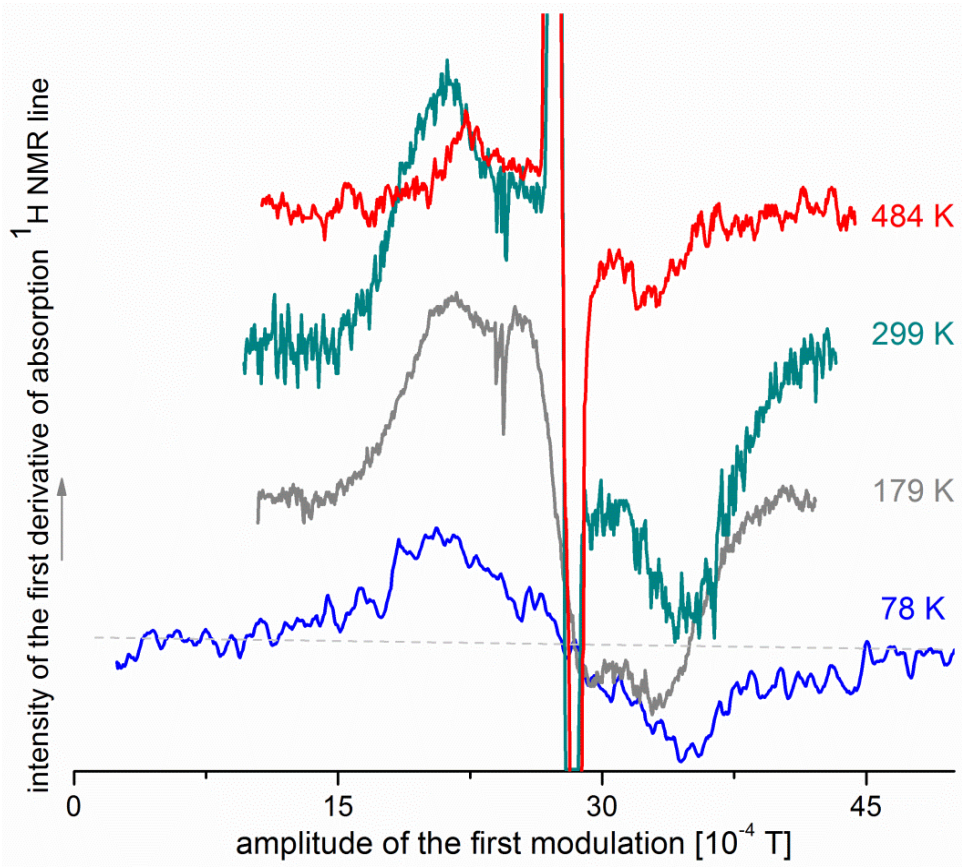

Figure 4 : Spectra of ^{1}H NMR line of PDA at different temperature.

ORIGINAL ARTICLE

decreased to $15.7 \cdot 10^{-8}$ T^2 at 160K, then over the temperature range from 261 K to 500 K it decreased continuously from 15.7 to $11 \cdot 10^{-8}$ T^2. Next, at the melting point the second moment of the ^{1}H NMR line decreased practically to zero, as shown in Figure 5.

In order to discuss the internal dynamics, the second moment of the ^{1}H NMR line was calculated according to the van Vleck formula[18] when the homo- and heteronuclear interactions were taken into account:

$$\mathbf{M_2^{rig} = \frac{3}{5}\gamma_H{}^2\hbar^2 I(I+1)\frac{1}{N}\sum_{j,k}^{N}\frac{1}{r_{H-H}^6} + \frac{4}{15}\gamma_N{}^2\hbar^2 S(S+1)\frac{1}{N}\sum_{j,k}^{N}\frac{1}{r_{H-S}^6}} \quad (2)$$

where: γ_I and γ_S are the gyromagnetic ratio of the resonance spin *I (hydrogen)* and non-resonance spin S (*nitrogen*), *N*-number of interacting spins, r_{jk}– inter-proton distance.

The motional process responsible for narrowing of the ^{1}H NMR lines was identified by comparing the experimental values of M_2^{exp} (1) with those M_2^{calc} calculated according to formula (2) for different models of internal motions.

The intermolecular reorientations that can modulate the Hamiltonian and in effect reduce the second moment of the ^{1}H NMR line are as follows:

- three-fold reorientation of both ammonia
- three-fold reorientation of the methyl group,
- two-fold reorientation of the cation,
- proton jump in hydrogen bond.

The onset of the molecular group reorientation around the distinguished axis with a frequency of an order of the ^{1}H NMR line width is the reason for the reduction in the second moment value from the low temperature value for the "rigid lattice" M_2^{rig} to M_2^{reo} according the equation:

$$\mathbf{M_2^{reo(1)} = M_2^{rig}\left(\frac{1-3\cos^2\gamma_{jk}}{2}\right)^2} \quad (3)$$

where γ_{jk} is the angle between the inter-proton vector in the molecular group undergoing reorientation and the axis of rotation[19].

The value of the second moment for jump motion between two minima is given by

$$\mathbf{M_2^{jump} = \frac{3}{5}\gamma_H{}^2\hbar^2 I(I+1)\frac{1}{N}\frac{a}{(a+1)^2}\sum_{j,k}^{N}\left[a\frac{1}{r_{H-HikA}^6} + \frac{1}{a}\frac{1}{r_{H-HikB}^6} + \frac{1}{r_{H-HikA}^3}\frac{1}{r_{H-HikB}^3}(3\cos^2\vartheta_{ikAB}-1)\right]} \quad (4)$$

where: the parameter $a = \exp\left(\frac{E_B - E_A}{RT}\right)$ depends on the depth of the nearest potential barrier E_A and E_B.

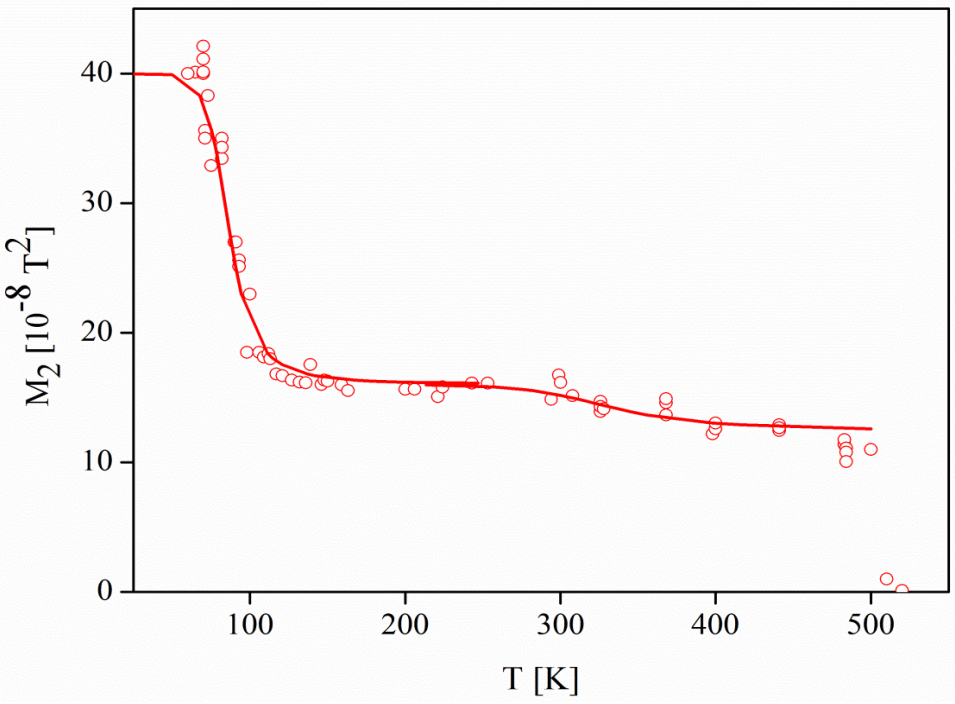

Figure 5 : Temperature dependence of the second moment of the ^{1}H NMR line of PDA.

ORIGINAL ARTICLE

X-Ray diffraction studies [CAD4 Express] performed at room temperature give various lengths of C-C and C-N bonds of the skeletons of the molecules in the elementary unit cell, typical to the molecular-ionic systems. Two subunits can be distinguished in the elementary unit cell. The calculated value of ^{1}H NMR M_2 for rigid lattice from the X-ray data is much higher (62.42 +2.23 or 62.75+2.09 $*10^{-8}T^2$) then the experimental ones. It can be explained by to short length of C-H and N-H bonds, while the hydrogen atom positions obtained from XRD results are charged with considerable error because of a low density of their electron clouds. Taking this into account, further calculations of the second moment were carried out for the C-H bond distance typical of methyl group, i.e. 1.09 Å and typical of ammonium group, i.e. 1.00 Å,[20,21], instead of 0.8899 Å and 0.8995 Å[18,19,22] as was also taking into account to previous studies of[23]. Just now, the inta and inter molecular contribution to the second moment of ^{1}H NMR line corresponding to the homo and hetero-nuclear interactions of the rigid structure was calculated as 40.1 $*10^{-8}T^2$, which is comparable to M_2=40$*10^{-8}T^2$ observed at 60 K. TABLE 6 collects the values of M_2 for the rigid lattice and calculated ones, assuming different types of internal motion, which subsequently were set on with the frequency of an order of a line width. One may take into consideration the set on of ammonia groups reorientation before the methyl groups, because their thermal displacement coefficient are higher than those of methyl (TABLE 2 and 3).

TABLE 6 : Calculated intra- and inter-molecular contribution to the second moment of ^{1}H NMR line of PDA.

Model of reorientation	Calculated values of the second moment of ^{1}H NMR line, M_2, in $10^{-8}T^2$		Experimental M_2 in $10^{-8}T^2$
	$M_2^{intra(1)(HH+NH)}$	M_2^{inter}	
Rigid structure	35.99+1.11	3	40 at *60K*
One ammonia group reorientation	31.51 +0.65	2.4	
Both ammonia group reorientation	27.07+0.13	1.8	
Methylgroup reorientation	18.76+0.13	1.3	
Conformational isomerisation	7.75+0.10	1.2	7.8 *at 250 K*
Jump of proton in hydrogen bond system	7.55 +0.10	1.2	
Isotropic reorientation	0	1	0 at *515 K*

The parameters of the thermally activated motion were calculated from the temperature dependence of the second moment of NMR line, according to the equation given by Kubo and Tomita[24]. The activation energy of methyl and ammonia group were estimated as 1.2 kcal/mol. The activation energy of axial reorientation of half of the cations from the elementary unit cell is 5.4 kcal/mol. It was assumed that the direction of the axis of the anisotropic reorientation of the cation is along the Cl—HN and Cl—HC hydrogen bonds. In Figure 5 is also given the calculated temperature dependence of the second moment for obtained activation energies of thee fold ammonium and methyl group reorientation as well as for whole organic cation motion, in agreement with the Kubo and Tomita equation.

CONCLUSION

We have investigated one of halogenoantimonates (III) with organic cation $[C_3H_{10}N_2]_2$ i.e. 1,2-propanediammonium pentachloroantimonate (III) dichloride. The crystals structure was determined at room temperature. On heating from 60K it undergoes "untrivial" phase transitions close to 261 and 355K. The set of on three fold reorientation of ammonia and methyl group was observed, with the activation energy of 1.2 kcal/mol, when undergoes with a frequency of an order of a few kHz. In high temperature phase the axial reorientation of half of the cations take place.

REFERENCES

[1] A.Pietraszko, B.Bednarska-Bolek, R.Jakubas, P.Zielinski; J.Phys.: Condens.Matter, **13**, 6471 **(2001)**.

[2] R.Jakubas, L.Sobczyk; Phase Trans., **20**, 163 **(1990)**.

[3] K.Uchino; Ferroelectric Devices, Marcel Dekker, New York, **(2000)**.

[4] J.Zaleski, R.Jakubas, L.Sobczyk, J.Mroz; Ferroelectrics, **103**, 83 **(1990)**.
[5] R.Blachnik, B.Jaschinski, H.Reuter, G.Kaster, Z.Kristallogr; **212**, 874 **(1997)**.
[6] R.Jakubas; Structure and Phase Transitions in Alkylammonium Halogenoantimonates(III) and Bismuthates(III), Wrocław University Press, Wrocław, **(1990)**.
[7] J.Zaleski; Structure, Phase Transitions and Molecular Motions in Chloroantimonates(III) and Bismuthates(III), Opole University Press, Opole, **(1995)**.
[8] L.Sobczyk, R.Jakubas, J.Zaleski; Pol.J.Chem., **(1997)**.
[9] G.Bator; Dielectric Relaxation and IR Studies on Phase Transitions in Alkylammonium Halogenoantimonates(III) and Bismuthates(III), Wrocław, **(1999)**.
[10] G.A.Fischer, N.C.Norman; Adv.Inorg.Chem., 41 **(1994)**.
[11] M.Bujak, J.Zaleski; J.Solid State Chem., **177**, 3202 **(2004)**.
[12] G.M.Sheldrick; SHELXS-97. Program for the Solution of Crystal Structure, University of G ttingen, Germany, **(1997)**.
[13] R.Jakubas, Z.Ciunik, G.Bator; Phys.Rev.B, **67**, 024103 **(2003)**.
[14] M.Bujak, J.Zaleski; Main Group Met.Chem., **25**, 583-584 **(2002)**.
[15] U.Ensinger, W.Schwartz, A.Schmidt; Z.Naturforsch., **38b**, 149-154 **(1983)**.
[16] M.Bujak, R.J.Angel; J.Phys.Chem.B, **110**, 10322-10331 **(2006)**.
[17] M.Bujak, R.J.Angel; Journal of Solid State Chemistry, **180**, 3026-3034 **(2007)**.
[18] J.H.Van, Vleck; Phys.Rev., **74(9)**, 1168 **(1948)**.
[19] C.P.Slichter; Principles of Magnetic Resonance, Springer Verlag, Berlin, Heidelberg, New York, **(1980)**.
[20] **(a)** The Cambridge Structural Database, F.H.Allen; Acta Cryst., **B58**, 380 **(2002)**; **(b)** Mercury CSD 2.0, C.F.Macrae, I.J.Bruno, J.A.Chisholm, P.R.Edgington, P.McCabe, E.Pidcock, L.Rodriguez-Monge, R.Taylor, J.van de Streek, P.A.Wood; J.Appl.Cryst., **41**, 466-470 **(2008)**; **(c)** Mercury, C.F.Macrae, P.R.Edgington, P.McCabe, E.Pidcock, G.P.Shields, R.Taylor, M.Towler, J.van de Streek; J.Appl.Cryst., **39**, 453 **(2006)**; **(d)** I.J.Bruno, J.C.Cole, P.R.Edgington, M.K.Kessler, C.F.Macrae, P.McCabe, J.Pearson, R.Taylor; Acta Cryst., **B58**, 389 **(2002)**; **(e)** F.Macrae; Acta Cryst., **B57**, 815 **(2001)**.
[21] A.I.Kitajgorodski; Krysztaly molekularne, PWN Warszawa, **(1976)**.
[22] J.Demaison, L.Margules, J.E.Boggs; Chem.Phys., **260**, 65-81 **(2000)**.
[23] W.Medycki, K.Holderna-Natkaniec, J.Swiergiel, R.Jakubas; Solid State Nucl.Magn., **24**, 209-217 **(2003)**.
[24] **(a)** R.Kubo, K.A.Tomita; J.Phys.Soc.Jpn., **9**, 888-919 **(1954)**; **(b)** H.S.Gutowsky, G.E.Pake; J.Chem.Phys., **18**, 162±170 **(1950)**; **(c)** T.P.Melia, R.Merrifield; J.Chem.Soc. A, 1166 **(1970)**; **(d)** T.P.Melia, R.Merrifield; J.Chem.Soc. A, 1259 **(1971)**.